

# Towards Optical Maritime Surveillance with High-Altitude Platforms

Jörg Brauchle, Ralf Berger, Tina Hiebert and Daniel Hein  
German Aerospace Center (DLR), Institute of Optical Sensor Systems, Berlin  
Email: {Joerg.Brauchle, Ralf.Berger, Tina.Hiebert, Daniel.Hein}@DLR.de

**Abstract**—Increasing importance and growing needs for monitoring and surveillance of maritime areas are a big challenge, in particular facing current solutions. Conventional aircraft are limited in operation time and range. Moreover, missions are cost-intensive for extended observations. Remote sensing satellites are suitable for scanning large areas, but they cannot continuously monitor a certain region of interest due to its orbit movement. This gap is going to be closed in the next years by *High Altitude Platforms* (HAP). HAPs are solar-powered unmanned aerial vehicles, which are capable to continuously operate for weeks or months at altitudes of between 15 and 20 kilometers. This enables long-term quasi-stationary applications while keeping the ability to relocate the platform within a certain range and time. The *German Aerospace Center* (DLR) researches and develops such a stratospheric platform within an integrated joint project. This aircraft is designed with a wingspan of 27 meters and a maximum take-off weight of about 138 kilograms. It includes a compartment to carry operational payloads with a weight of up to 5 kilograms.

This article presents a design of an integrated optical payload system specially tailored to this undergoing development platform. The aim of this novel technology payload is to provide new applications in the field of maritime remote sensing safety and security. The payload fulfills general high-altitude operation requirements. Amongst others this comprises the operation within a wide temperature spread between night / daylight conditions and the on-board real-time image processing at a maximum power consumption of 70 watts in total.

Requirements of a HAP-based optical payload system are shown. A design fulfilling these requirements and the communication concept using both, the narrowband and broadband data link, are presented. Furthermore, AI image on-board processing approaches and its application for maritime purposes are discussed.

## I. MOTIVATION

Given the ever-increasing amount and importance of traffic at sea, a comprehensive and up-to-date maritime situation picture is a fundamental requirement for the safe and secure operation of maritime traffic and infrastructures. This also requires broad surveillance of such infrastructures and traffic routes for possible disturbances as well as tracking of maritime traffic participants. For these tasks, different technical systems are used nowadays.

In coastal areas and in technical infrastructures, e.g. harbours, static traffic detection systems based on radar and cameras are mainly applied. In addition, ship data is collected via the *Automatic Identification System* (AIS) from satellites or shore-based stations and transmitted to central *Vessel Traffic Services* (VTS) [1].

However, outside of infrastructure-based monitoring, there are significant gaps in the situation picture. For example, AIS can be intentionally turned off, e.g. to disguise criminal activities such as dumping, smuggling and illegal fishing. In addition, smaller boats usually do not send AIS signals at all. Also dangerous flotsam like fallen containers are not detected in this way. Last but not least, there are situations and environmental conditions where conventional systems such as AIS or radar provide only insufficient or inconsistent data [2].

In such cases, optical surveillance systems (satellite-based, but primarily airborne) make a substantial contribution to complementing the maritime situation picture. Various such systems and platformers have already been in operations for many years. For example, some European countries as well as *European Maritime Safety Agency* (EMSA) use dedicated aircraft and drones in addition to satellite data for surveillance of vessel movements, maritime pollution control or *search and rescue* (SAR) missions [3].

Satellites have the advantage of global coverage, aircraft systems can be flexibly instrumented and manoeuvred. Drones achieve comparably long operation times. What all systems have in common, however, is that they can only observe an area episodically for a limited period of time. Between those revisits, there is a kind of a "blind spot." In particular, continuous tracking of vessels or objects in the water is only possible to a limited extent.

This is where a *High Altitude Platform* (HAP, sometimes also referred to as *High Altitude Pseudo Satellite* HAPS) can fill a critical capability gap. Such systems, usually solar-powered stratospheric gliders with mission durations in the range of weeks to months, combine increased resolution and manoeuvrability with the ability to persistently observe a relatively large area.

The possibility of such a persistent observation capability may be a tremendous enhancement to maritime situational awareness in the future. What is needed for application are operationally usable HAPs. The proposal of an appropriate optical sensor system and detection technologies designed for the specific characteristics of such a carrier are subject of this article.

## II. PREPARATORY WORK

In the past years several real-time airborne imaging systems were developed and demonstrated [4]. A real-time aerial



Fig. 1. Aircraft with DLR *Modular Airborne Camera System (MACS)* and WiFi-based 10 MBit/s data downlink.

camera system in the context of maritime security applications was demonstrated in 2016 on the *EMSec* verification experiment [5], [6]. The instrument comprised a multi-sensor *Modular Aerial Camera System (MACS)* combined with a 5 GHz broadband downlink installed into a DLR research aircraft Dornier 228 (see figure 1). Processing all four spectral-different sensors, a real-time detection for non-water objects was demonstrated. Ships and simulated water pollution was detected automatically. The broadband datalink was used to send images to the ground control station, where a full resolution real-time map was generated. This map was augmented with positions of the automatically detected water objects (see figure 2). In this experiment a object detection completeness of 95% was shown, while the correctness reached a level of 53%. The absolute positional accuracy of the projected real-time imagery resulted in 2 meters without post-processing of images or navigation data. The broadband datalink was capable to transmit image data in real-time over a distance of up to 50 kilometers.

In a joined effort of DLR and the first response organization *International Search and Rescue Germany (I.S.A.R.)* a miniaturized version of this MACS camera system was developed to enable real-time mapping using small UAVs for mobile search and rescue applications (see figure 3) [7], [8]. This single-sensor camera was integrated into a *vertical take-off and landing (VTOL)* electric powered fixed wing UAV with a *maximum take-off weight (MTOW)* of 14 kilograms (see figure 4). The overall system is capable to autonomously operate up to 1.5 hours with a ground speed of up to 80 kilometers per hour. This enables autopilot-supported capturing of rather large areas within a short time - without any need for landing strips or airports. An integrated broadband link enables real-time image transmission within a range of up to 10 kilometers to instantly project images mosaics. The camera system itself weighs about 1.5 kilograms and has a power consumption of about 30 watts including broadband radio transmission.

In a next step, the system will be downsized for a 7.4 kilo-



Fig. 2. Generation of seamless aerial maps from the transmitted image data in real-time. The latency between image acquisition and visualization is about two seconds, the positional accuracy in the range of 2 meters.



Fig. 3. UAV-based real-time aerial camera system for mapping with a total weight of about 1.5 kilograms. The sensor is interchangeable with visual, near-infrared and thermal-infrared sensor.



Fig. 4. Fixed wing VTOL-UAV with a maximum total weight of 14 kilograms and a wingspan of 3.5 meters including down oriented aerial camera.



Fig. 5. DLR HAP solar-powered stratospheric platform (rendering).

grams MTOW fixed wing UAV. The camera payload is designed with a weight of about 680 grams including a 50 MPix sensor and a power consumption of approximately 25 Watts.

### III. HAP DEMONSTRATOR

In a joint project the DLR develops a HAP, an appropriate optical sensor system and a ground station to operate and control the system. All elements are developed concurrently. With respect to carrier and payload, primarily to reduce weight and power consumption. This is done by considering the requirements of the counterpart and making use of synergies by sharing devices. The platform is a solar-powered heavier-than-air glider designed to have a wingspan of 27 meters and a weight of 138 kilograms (see figure 5). The mission altitude is approximately 20.000 meters above sea level. During night the platform does not descend below 15.000 meters keeping distance to turbulent weather conditions and having the ability to re-climb to the mission altitude during morning hours.

The payload is mounted at the fuselage's nose and covered by a technical fairing comparable to tent fabric (see figure 6). Controlled by an inlet flap, air flows guided through the compartment to cool down critical components.

Two radio datalinks are provided. One is a link dedicated to the payload and for energetic reasons only working during missions. The link operates in the X-Band with a frame-based CCSDS protocol implemented. Under best conditions this satellite-class link provides a gross data rate of approximately 100 Mbit/s unidirectional. Without having field experience yet a net throughput of approximately 60 Mbit/s is assumed.

A second link is the *command & control* (C2) datalink which is used to fly and control the platform. This bidirectional link is permanently accessible and operates in the S-Band. It provides a throughput of approximately 1 Mbit/s. In most situations the available data rate is not fully utilized. Remaining budget is used with lower priority for payload purposes. Particularly, these are sending acknowledges establishing an X-Band return channel and receiving health monitoring information during the night. For the test phase on locations around the world, a portable ground station provides communication from and to the HAP in a radius of approximately 250 kilometers.

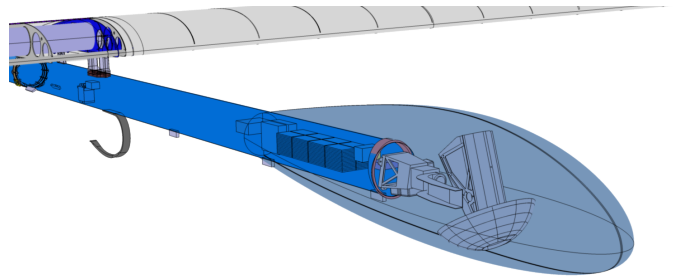


Fig. 6. HAP payload compartment at the front side of the fuselage (illustration). Covered by fabric with an open area at the bottom.

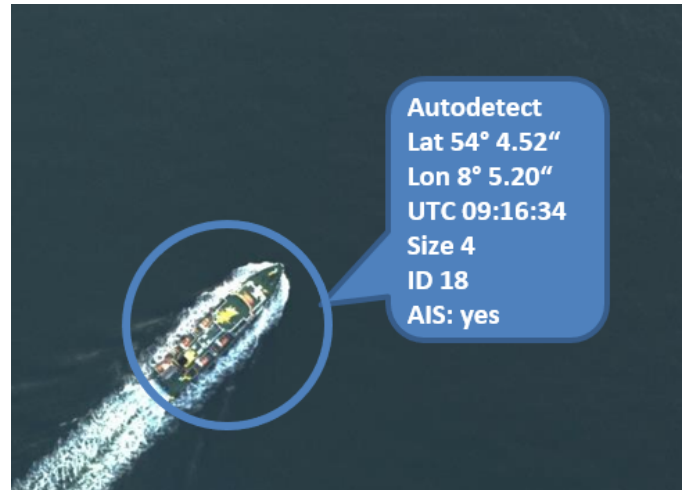


Fig. 7. Autodetecting non-water objects: Only annotated information is sent to the operator who retrieves the corresponding image if necessary.

### IV. HAP OPTICAL INSTRUMENT

Operating an aerial camera on a HAP requires some unusual specification. Most importantly, weight and power consumption must be reduced to a minimum. Persistent hovering over a region of interest in an altitude of 20.000 meters requires the ability to independently point into a certain direction. Introducing a two-axes gimbal lets the camera move around roll and pitch to provide this functionality. Additionally, manoeuvres can be compensated. Thus, the aircraft can be adjusted to minimize energy consumption and to maximize solar impact.

Two modes of operation are enabled which are shown in figure 8. First, pointing to a geolocation lets the user follow an object achieving high time resolution of a location. Second, mosaicking lets the system scan an area and projects one georeferenced image seamless next to the previous image. This mode is intended to cover large areas to search for non-water objects and can highly automated implemented using object-based or AI-based classification (see V Data Processing). In case of automatically detected non-water objects the system alerts. The operator makes a decision based on the corresponding image(s). Alternatively, the arising mosaic can be used to feed a situation map (figure 9). The MACS-HAP gimbal provides off-nadir deflections of +/-30 degree around roll and

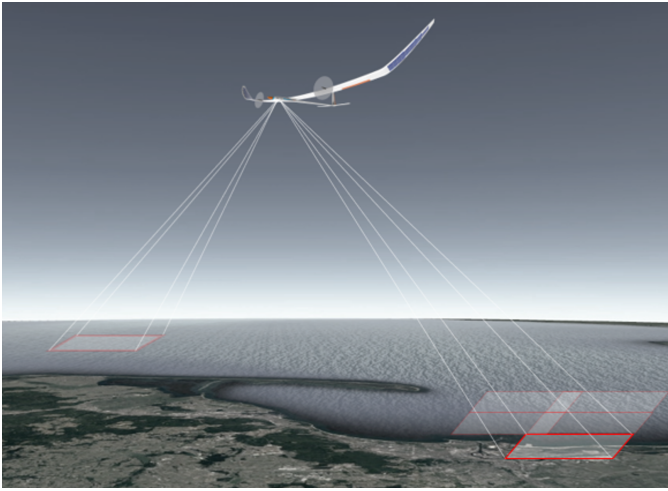


Fig. 8. Pointing mode (left) lets the observer track an object and provides high time resolution. Mosaicking (right) scans an area for non-water objects and provides large area coverage.

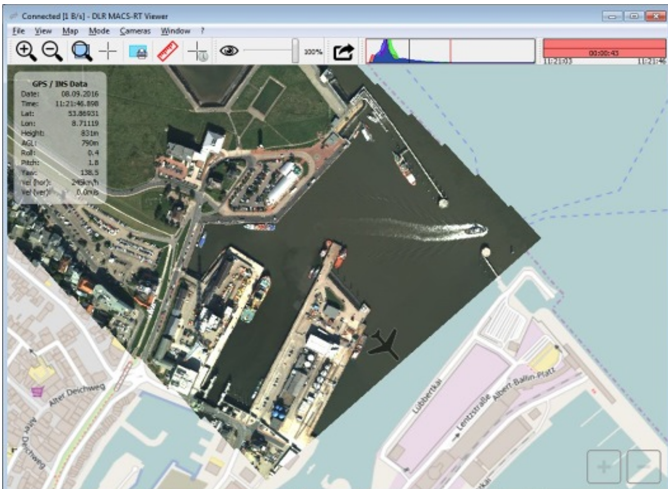


Fig. 9. Instant transmission of georeferenced images provides a mosaic which can be enriched with information of other sources yielding to a situation map.

pitch, respectively. Thus, an area of approximately 530 square kilometers is covered. Figure 10 shows the rotatable mounted camera. A spherical cover is attached filling the gap between the optic's frame and the payload compartment fairing to avoid turbulences and undefined cold air flow.

Recent work concluded, that a ground resolution of 15 to 20 cm is necessary to recognize small non-water objects like dinghies or wreckage [5]. In conjunction with a  $3.76 \mu\text{m}$  pixel pitch focal plane this requirement yields to a focal length of 500 mm. The optical performance (e.g. contrast and *optical transfer function* (OTF)) is increased by avoiding shadowed regions. Such regions arise in the image centre when a holed mirror is used to collect and reflect light, see e.g. Cassegrain telescopes. As a result, a refractive-only design is chosen, see figure 11. The setup contains a front glass with infrared-cutting coating, five lenses in two groups, a fold mirror and a 150 MPix camera body. The fold mirror is optically inactive

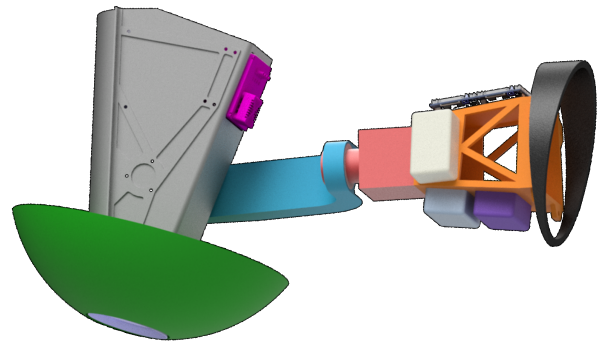


Fig. 10. Components of DLR MACS-HAP aerial camera. Optical part can be rotated around roll and pitch. The sphere closes the gap between instrument and fairing.

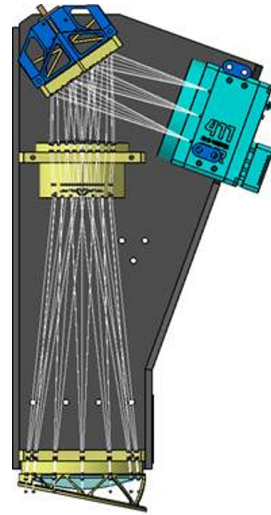


Fig. 11. The optical device has a focal length of 500 mm and consists of one front window, five lenses, a fold/defocus mirror and a 150 MPix sensor.

but provides the capability to be moved perpendicular to the mirror plane. This lets the focus be adjusted in case of pressure or thermal effects on the optical path and eliminates the need for athermal design. Additionally, the mirror reduces instrument height to minimize inertia moments the gimbal has to accelerate. The most important optical and environmental specifications are shown in table I.

## V. DATA PROCESSING

A single image of the 150 MPix @ 12 bit sensor has a raw data footprint of 225 MByte. Depending on operation mode and capturing task, a trigger interval in the range of two seconds is foreseen. Thus, the sensor will require a large amount of raw data to be handled and processed. Two approaches are going to be applied to face these data volumes: Firstly, the application of artificial intelligence and deep learning methods to automatically analyse and detect relevant image data (anomaly detection). Secondly, the application of compression algorithms to maximize the image data throughput via the broadband downlink.

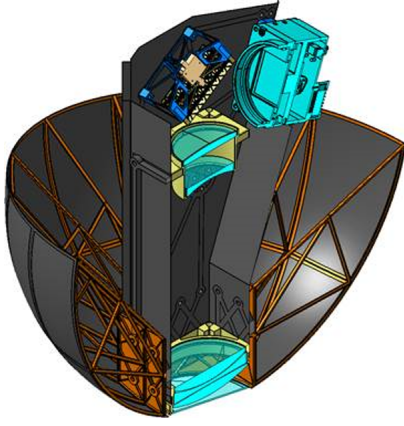


Fig. 12. Cut through the sensor device showing the optical elements and the structure carrying the sphere.

TABLE I  
AERIAL CAMERA MAIN SPECIFICATIONS

Specification	Value
GSD nadir @ 20 km	15 cm
Focal length	500 mm
F-Number	6
# of pixels per image	150 MPix
Pixel pitch	3,76 $\mu\text{m}$
Aperture	85 mm
Field of View	6.1° x 4.6°
Of-nadir pan/tilt angle	+/- 30°
Spectrum VIS/NIR	400 - 900 nm
Weight of whole system	5 kg
Dimensions (LxHxW)	640 x 370 x 340 mm <sup>3</sup>
Max. operating Temperature	+40 °C
Min. operating Temperature	-20 °C
Air pressure min.	25 mbar

### A. Anomaly detection

Most of the data is non-informative for commercial or scientific use, so an on-board approach to detect the relevant data and compressing the non-informative data at a higher rate can be used to reduce the data downlink throughput. Anomaly detection can be utilized to identify the relevant data. An anomaly can be defined as anything that does not match an expected pattern. In the case of maritime surveillance, ships are considered as anomalies and water as normal class.

Such anomaly detection can be accomplished using an autoencoder, a neural network consisting of an encoder and a decoder. The encoder maps the input data to its latent representation. The decoder maps the representation back to the input data.

For the task of anomaly detection an autoencoder is trained to reconstruct its input using a loss functions that aims to minimize the reconstruction error. The training is semi-

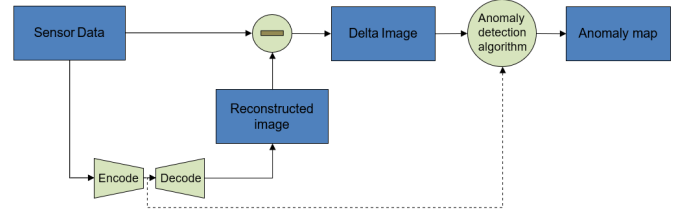


Fig. 13. Pipeline for anomaly detection with autoencoders. The detection algorithm can either be based on the delta image, or on the encoding representation itself.

supervised with training data only comprising data from the normal class. As a result the reconstruction error of anomalous data is significantly higher than the reconstruction error of normal data when the autoencoder is applied to test data. The reconstruction error, visualized in the delta image, can then be used to identify the anomalies by applying an anomaly detection algorithm (see figure 13, solid line). This algorithm must be adapted to the specific data and detection task. It can be a threshold algorithm but may include further image processing. The output of the anomaly detection algorithm is an anomaly map, a binary mask that marks anomalous regions of the source image.

Alternatively, only the encoder part of the autoencoder is applied to the test data (see figure 13, dashed line). Anomalies will generate latent representations that deviate from the representations of the normal class. By applying an anomaly detection algorithm to this encoded features the anomaly map can be retrieved. Differences between the encoded features of the anomalies and normal class in the test data can be evaluated here as well as their deviations from the encoded features learned during training [9].

### B. Compression

In order to match the bandwidth limitations of the data downlink and to optimize the image data transmission, the images are going to be compressed. Generally spoken, there are two types of compression methods applicable for images: lossless and lossy compression algorithms. Lossless compression, such as Lempel-Ziv methods and its variations are quite inefficient for raw image data [10]. They have a large computational footprint and reduce data size of raw images typically by just 5% to 10% (compression ratio of about 10:9) due to sensor noise. On the other hand, conventional lossy image compression algorithms, such as JPEG or WebP achieve higher compression ratios, but are limited to a colour depth of 8 bit [11], [12]. In contrast, the designed system will apply a frequency-domain lossy compression based on the JPEG algorithm, but with a supported bit depth of 12 bits [13]. Thus, compressed images maintain full radiometric and geometric resolution. At the same time, this algorithm typically reaches a compression by up to 95% (ratio of about 20:1), depending on image content and compression quality settings.

## VI. CONCLUSION

Maritime applications are affected by large observation extents and missing infrastructure. Conventional aircraft and remote sensing satellites cover certain tasks, but leave blind spots due to technical limitations and operating costs for long-term surveillance missions. A HAP may constitute a suitable supplement. It is shown that this technology in combination with a suitable remote sensing payload is capable to provide high-resolution aerial imagery of regional areas for weeks and months. However, the technical requirements of a HAP are exceptional. The mechanical construction of the platform itself, the design of an appropriate high-precision optical payload with respect to the given power and mass limits, the data handling and automatic processing of such an amount of image data is demanding. The German Aerospace Center develops both a carrier and an optical instrument. This article presents an optical payload design providing a ground sampling distance in the range of 15 centimetres together with a data processing concept which may meet the facing demands. It includes a gimbal, a refractive optic, a 150 MPix sensor and a computational stack for artificial intelligence and deep learning methods to automatically detect objects of interest. Two data links enable remote control, extracted information transmission and broadband image transmission between the HAP and a ground control station.

## VII. OUTLOOK

In the next steps the refractive optic including fold, sensor and frame will be assembled, adjusted and quality-measured. The defoc mirror is to be implemented and tested to focus the rays even in normal laboratory environment at ca. 1015 mbar and 21 °C. The gimbal acceleration performance is tested and then mass-optimized for the final design. First radiolink field tests will be conducted to be ready for a test flight. The *critical design review* (CDR) is scheduled in the year 2022. Compute stack including AI-accelerator will be qualified and tested in environment comparable to the expected conditions, particularly with respect to thermal balancing, pressure and cosmic radiation. In parallel, the autoencoder is trained further to achieve better reconstruction and detection results.

## REFERENCES

- [1] P. Last, "Analysis of automatic identification system data for maritime safety," Ph.D. dissertation, 2017. [Online]. Available: <http://urn-resolving.de/urn:nbn:de:gbv:579-opus-1006908>
- [2] Y. Zardoua, A. Astito, and M. Boulaala, "A comparison of ais, x-band marine radar systems and camera surveillance systems in the collection of tracking data," 04 2020.
- [3] European Maritime Safety Agency, "Emsa outlook 2020," 2020. [Online]. Available: <http://www.emsa.europa.eu/publications/item/3890-emsa-outlook-2020.html>
- [4] P. Scherbaum, J. Brauchle, T. Kraft, and S. Pless, "MACS-Mar - a real-time capable multisensor remote sensing system for maritime applications," in *ICARES 2015*, ser. IEEE International Conference on Aerospace Electronics and Remote Sensing, IEEE, Ed. Curan Associates, Inc, Dezember 2015. [Online]. Available: <http://elib.dlr.de/103496/>
- [5] J. Brauchle, S. Bayer, and R. Berger, "Automatic ship detection on multispectral and thermal infrared aerial images using MACS-Mar remote sensing platform," in *Pacific-Rim Symposium on Image and Video Technology (PSIVT 2017)*, S. Satoh, C.-W. Ngo, and J. Yuan, Eds. Springer Science, November 2017. [Online]. Available: <http://elib.dlr.de/118512/>
- [6] J. Brauchle, S. Bayer, D. Hein, R. Berger, and S. Pless, "MACS-Mar: A real-time remote sensing system for maritime security applications," *CEAS Space Journal*, pp. 1–10, April 2018. [Online]. Available: <https://elib.dlr.de/121263/>
- [7] D. Hein, T. Kraft, J. Brauchle, and R. Berger, "Integrated UAV-based real-time mapping for security applications," *ISPRS International Journal of Geo-Information*, vol. 8, no. 5, p. 219, 2019. [Online]. Available: <https://www.mdpi.com/2220-9964/8/5/219/pdf>
- [8] D. Hein, S. Bayer, R. Berger, T. Kraft, and D. Lesmeister, "An integrated rapid mapping system for disaster management," *The International Archives of Photogrammetry, Remote Sensing and Spatial Information Sciences*, vol. 42, p. 499, 2017. [Online]. Available: <https://core.ac.uk/download/pdf/84276342.pdf>
- [9] D.-M. Tsai and P.-H. Jen, "Autoencoder-based anomaly detection for surface defect inspection," *Advanced Engineering Informatics*, vol. 48, p. 101272, 2021. [Online]. Available: <https://www.sciencedirect.com/science/article/pii/S1474034621000276>
- [10] S. Naqvi, R. Naqvi, R. A. Riaz, and M. F. Siddiqui, "Optimized RTL design and implementation of LZW algorithm for high bandwidth applications," *Przeglad Elektrotechniczny*, vol. 87, pp. 279–285, 2011.
- [11] N. Verma and P. Mann, "Survey on JPEG image compression," *International Journal of Advanced Research in Computer Science and Software Engineering*, vol. 4, pp. 1072–1075, 01 2014.
- [12] Richard Rabbat, "WebP, a new image format for the web," 2010. [Online]. Available: <https://blog.chromium.org/2010/09/webp-new-image-format-for-web.html>
- [13] Independent JPEG Group (IJJ), "libjpeg C library," <http://ijg.org/>, 2018.